ORIGINAL ARTICLE

lajss.org© Latin American Journal of Solids and Structures

www.lajss.org

The Seismic Behavior of Block Type Deep Soil Mixing

Mahsa Moradi Shaghaghi[a]*, Iradj Mahmoudzadeh Kani[a], Hassan Yousefi[a]

[a]School of Civil Engineering, College of Engineering, University of Tehran, Tehran, Iran. E-mails: m.m.shaghaghi@ut.ac.ir, imkani@ut.ac.ir, hyosefi@ut.ac.ir

*Corresponding author

https://doi.org/10.1590/1679-78256439

Abstract

Deep soil mixing method (DSM) is a novel in situ technology in soil improvement in which different cementitious materials are mixed with soil and form a soil-cement column with improved engineering characteristics. Due to the configurations of these improved soil-cement columns, different types of DSM are formed, such as wall type, grid type, block type, etc. Due to the expansion in the construction of massive industrial structures, the use of block type DSM to control the settlements has grown. In order to use this soil improvement under the foundation of different structures, it is essential to study the seismic behavior of this mixture using site response analysis and wave propagation. In this paper, the seismic behavior of block type DSM is studied through fully nonlinear analyses. Nonlinear soil is modeled using the overlay method, which uses the parallel element modeling concept. Whereas, the DSM is modeled with elastic perfectly plastic behavior. It is observed that utilizing block type DSM has positive effects in seismic response of the soil layer, such as a considerable reduction in surface response acceleration.

Keywords

block type deep soil mixing (DSM), soil improvement, seismic behavior, soil-cement mixture, nonlinear analyses, overlay method, Mohr-Coulomb criterion, surface response acceleration

Graphical abstract

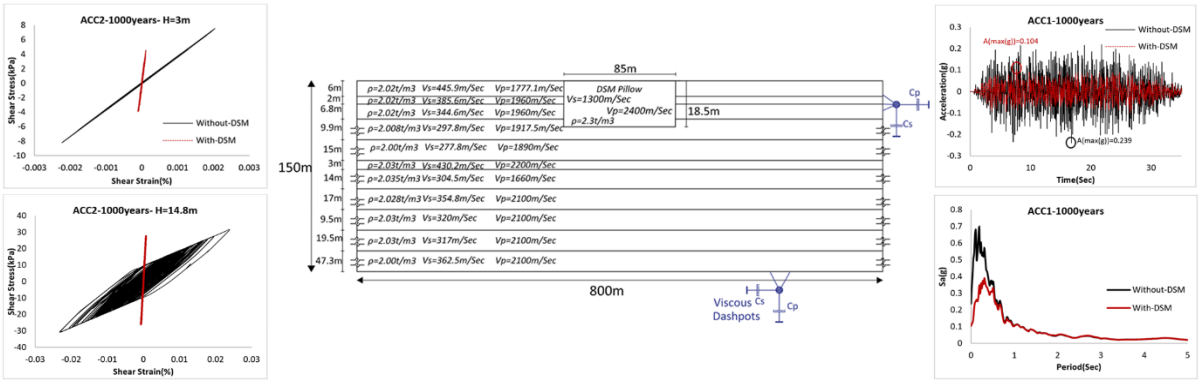

Received: February 07, 2021. In revised form August 17, 2021. Accepted August 26, 2021. Available online September 08, 2021.
https://doi.org/10.1590/1679-78256439

1. Introduction

The deep soil mixing method (DSM) is an in situ soil improvement technology in which the soil is mixed with cementitious and other materials, these materials are called “binders” and they are in either slurry or dry forms. These materials are injected through hollow, rotated mixing shafts tipped with some type of cutting tool that forms a hard column of treated soil in different shapes such as block, wall, lattice, and column configurations (See Fig. 1). The methods in which dry binder is blown pneumatically into the ground are called the dry method of deep mixing. The dry method uses mechanical mixing which consists of vertical rotary shafts with mixing blades at the end of each shaft. Binder is injected into the ground in the penetration and withdrawal stage. The mixing blades rotate in the horizontal plane and mix the soil and the binder. In this operation, a column of improved soil is constructed in the ground. While, the techniques in which binder-water slurry is pumped into the ground are generically called the wet (slurry) method (Kitazume and Terashi 2013). In comparison to the soil before treatment, the soil-binder composite material has enhanced engineering properties such as increased strength, lower permeability, and reduced compressibility; however, this cement-treated soil is in the category of brittle materials with high stiffness and strength but low residual strength (FHWA-RD-99-138 2000; FHWA-HRT-13-046 2013; Liu et al. 2012; Yapage et al. 2015).

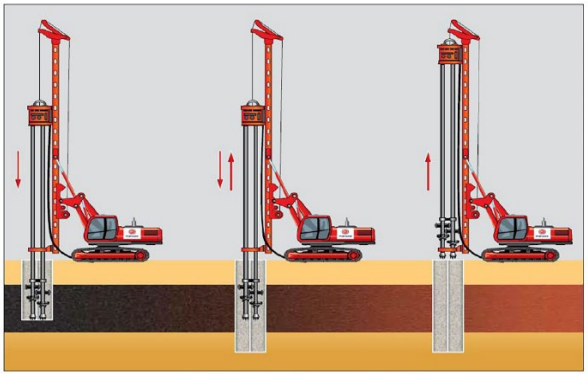

Fig. 1. Schematic deep soil mixing procedure

The main applications of DSM are reinforcing, strengthening, deformation control of foundation soil, liquefaction mitigation in areas prone to earthquake and settlement reduction. Moreover, this method is used in the hydraulic cut of walls, used to prevent water movement through or under retaining structures and into excavations below the water table. Another use of DSM is to remediate environmentally hazardous materials trough stabilizing contaminated soils. The improved specifications of these enhanced soil columns depend on the soil properties, quantity and characteristics of the cementitious materials, construction variables, loading and other operational parameters (FHWA-HRT-13-046 2013; O’Rourke and McGinn 2006).

Design methods for soil-cement mixes, as structural foundations, are not as well developed for seismic loadings as those for static loadings. Thus, the seismic behavior of DSM and the superstructure should be studied carefully (Khosravi et al. 2016).

Some studies have investigated the seismic behavior of these improved soil mediums with deep soil mixing methods of different types. Kitazume and Terashi (2013) investigated the response of different types of deep soil mixings constructed in various parts of Japan to strong ground motions. They reported that in the Tohoku earthquake (2011, Japan), no damages were found in the improved soil by the DSM and the superstructures, while in the parts without improvement, serious damages were identified. These researchers concluded that the soil treatment by DSM demonstrates a proper performance and applicability for mitigating damages caused by strong ground motion to the ground and superstructure while they were subjected to a large seismic force. Yamashita et al. (2018) investigated the seismic behavior of piled raft foundation with and without deep mixing walls. They demonstrated that the acceleration response spectra amplification of the raft with deep mixing walls (DMW) was significantly lower than the case without DMW in long periods. Besides, they stated that the ground displacements in the cases without deep mixing walls were bigger than those with deep mixing walls.

Bradley et al. (2013) studied the effects of lattice-shaped treatment of the soil on the seismic behavior of the soil medium. They indicated that while lattice-shaped ground treatments in all geometries were effective in reductions of peak surface displacements and vertical settlements of the soil, an increase in the amplitude of the surface ground motion and acceleration spectra was observed. Namikawa et al. (2007) studied the dynamic behavior of soil-cement reinforced walls. They indicated that concentrated tensile stress occurred at the mid-length and corner of these lattice-

shaped improved walls. It was noted that these improvements have positive effects on the liquefaction potential of the soil layers. Moreover, they indicated that soil-cement improved walls might experience partial failure during intensive earthquakes; however, with this partial failure, the displacement of unimproved soil does not increase significantly. This partial failure will reduce the restraining effects of improved soil, but it does not affect liquefaction mitigation of improved soil unless the failure is severe. Khosravi et al. (2016) conducted large centrifuge tests to evaluate the seismic response of grid type soil-cement reinforcement. They showed that the soil without any reinforcement experienced sever nonlinearity in strong shakings but using reinforcement decreased this nonlinearity. On the other hand, adding reinforcement to soil increased the stiffness of the site, and this resulted in stronger accelerations at the ground surface for different input motions.

In most of the conducted researches, the behavior of grid and wall type deep soil mixing, which are mostly used in mitigating soil liquefaction potential, was studied. However, the seismic behavior of block type deep soil mixing improvements used in the foundation soil of the massive structures such as industrial structures to control the settlements, are not studied in detail. Therefore, a comprehensive study is required for a complete understanding of the behavior of the soil domains enhanced with block type deep soil mixing method. In this paper, the nonlinear seismic behavior of the block type deep soil mixing (known as DSM pillow) is studied for a site with different layers and properties. In this type of improvement, a uniform improved soil block is formed by overlapping DSM columns. This method results in the most stable soil in comparison to the other DSM types, and it is used to reduce the settlements. The application of DSM pillow is inevitable in some massive industrial structures with large settlements since in most cases it is more economical than other methods of reducing settlements.

The first part of this paper is devoted to the finite element modeling details and generating input ground motions. In the second part, the effects of the DSM pillow with specific characteristics on the surface acceleration, surface response acceleration spectrum and shear stress-shear strain loops are studied.

2. Finite element modeling

The simulation of the SH waves propagation in a 2D isotropic homogeneous medium is described in this part. The dynamic analyses of the soil domain are performed in the time domain. The vertically propagating shear waves (SH waves) are studied in the analyses. Thus, input ground motion is applied in the horizontal direction, solely. The finite element models of the soil and the DSM pillow are created by ABAQUS finite element software (Simulia Abaqus 2018). In order to figure out the effects of the block type DSM with a specific constant width, the model is assumed to be two dimensional.

There are three general approaches to modeling soil behavior in site response analyses. The first and simplest method is to assume linear stress-strain behavior for soil layers. This approach may be reasonable in very small strain ranges. In large earthquakes, however, the soil is known to demonstrate nonlinearity. In this phase, the shear modulus of the soil decreases, and the hysteresis damping increases with the increase in the shear strain. The second method in site response analysis is the equivalent-linear approach. In this type of analysis, the shear modulus and damping of the soil are adjusted in an iterative approach using modulus reduction and damping curves. It should be noted that this approach is an approximation of fully nonlinear analysis, and it is not suggested in high strain levels (Kaklamanos 2012; Kaklamanos et al. 2014; Kaklamanos et al. 2015a; b, Bolisetti 2014; Thompson et al. 2012; Zalachoris and Rathje 2015).

The third approach, which is the most accurate method, is fully nonlinear analysis. This analysis is carried out in the time domain. In this approach, rather than using a single value of shear modulus and damping, a fully nonlinear analysis allows for a more precise demonstration of the true cyclic stress-strain path by tracing the stress-strain path of the hysteresis loop during the earthquake (Kaklamanos 2012; Bolisetti et al. 2014). The fully nonlinear approach is utilized in this study for the sake of accuracy. Different methods exist for modeling nonlinear behavior of soils. One of the most applicable models which can be implemented in a wide range of finite element codes readily is the overlay model (Kaklamanos 2012; Kaklamanos et al. 2014; Nelson and Dorfmann 1995). The overlay model uses parallel load-carrying elements with different stiffness and yield stress, to model the behavior of a backbone stress-strain curve. The parallel model of Iwan (1967) and Mroz (1967) has been used in different soil dynamic studies. This method can be applied to 2D and 3D models, easily. In this model, the stress-strain behavior of the material is modeled using a set of elastoplastic parallel elements with varying stiffness and yield stress (Kaklamanos 2012; Kaklamanos et al. 2014; Kaklamanos et al. 2015a; Fares 2019). The soil medium used in this study consists of 11 layers with different characteristics that are related to a specific site. The characteristics of these layers are illustrated in the Table 1. The stress-strain backbone of each layer is obtained using modulus reduction (G/G_{max}) and damping curves of layers (Kramer 1996). G/G_{max} and ξ of each layer are demonstrated in Fig. 2 according to the corresponding degradation curves. The characteristics of soil layers are obtained from the comprehensive geotechnical tests conducted in the field at the site of new units of a power plant in west Asia.

The DSM used in this study is modeled using the Mohr-Coulomb failure criterion, which is a linearly elastic-perfectly plastic model. In this study, DSM block is constructed with the placement of several soil-cement columns with diameter of 1.6m and coverage of 20% with the depth of 18.5m. It should be noted that the maximum achievable depth for the DSM technology with currently available machines is about 20-25 m. In the second part of this paper, the seismic behavior of improved soil with specific material and geometric properties is studied. These properties are presented in Table 2.

Table 1 Soil profile at specific site used in analyses

No. Layer	Thickness (m)	Depth (m)	Density $\rho(t/m^3)$	S-wave velocity $V_S(m/\sec)$	P-wave velocity $V_p(m/\sec)$	Degradation Curves
1	6	6	2.02	445.9	1777.1	A
2	2	8	2.02	385.6	1960	B
3	6.8	14.8	2.02	344.6	1960	C
4	9.9	24.7	2.008	297.8	1917.5	C
5	15	39.7	2.0	277.8	1890	D
6	3	42.7	2.03	430.2	2200	D
7	14	56.7	2.035	304.5	1660	D
8	17	73.7	2.028	354.8	2100	E
9	9.5	83.2	2.03	320	2100	E
10	19.5	102.7	2.03	317	2100	F
11	47.3	150	2.0	362.5	2100	F

Table 2 Different characteristics of improved soil used in analyses

DSM	Density $\rho(t/m^3)$	S-wave velocity $V_S(m/Sec)$	P-Wave velocity $V_p(m/Sec)$	Friction angle $\varphi(^\circ)$	Cohesion C (KPa)	Length (m)	Thickness (m)
	2.3	1300	2400	0	1000	85	18.5

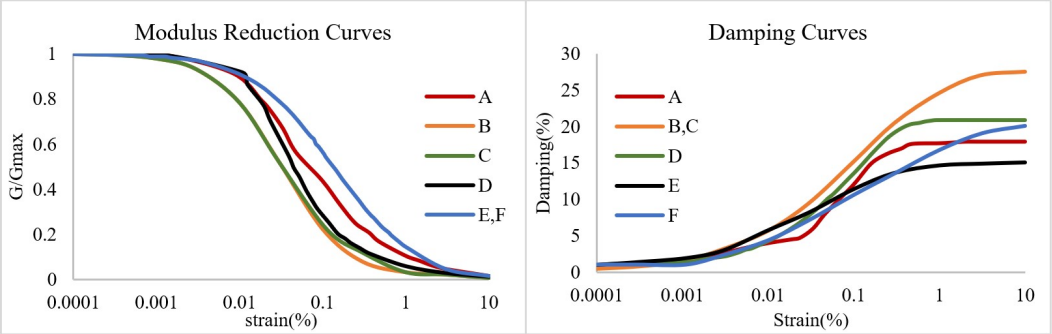

Fig. 2. Shear modulus reduction and damping curves of different layers of soil

The soil and soil-cement mix are meshed using plain strain 4-node bilinear, reduced integration with hourglass control elements (CPE4R). In order to determine the maximum mesh size, the general rule of specifying ten elements per wave-length should be considered in every wave propagation finite element model (Alford et al. 1974). In this study, the element size of 3m is used in the analysis. The authors checked the sensitivity of the analyses to the mesh size finer than 3m by applying mesh size equal to 1.5m. The result of the two mentioned cases had differences of less than 5%. Thus, it is logical and appropriate to use elements with a size of 3m.

Generally, each nonlinear soil model contains two types of damping, which are viscous (small-strain) damping and hysteresis damping. Hysteresis damping is related to the energy dissipation while loading and unloading cycles (Hashash et al. 2010). In the models that follow Masing loading-unloading rules (Masing 1926) like the overlay model used in this paper, hysteresis damping is proportional to the area inside hysteresis loops, and it is automatically considered with loading and unloading steps of the analyses. There is no need to specify extra features in the model. However, some studies have demonstrated that utilizing the Masing rule may cause some over-damping in large strains. The other type of damping is viscous damping, which is damping related to small strains. In other words, most of the models available for nonlinear soils give nearly zero damping in small amounts of the soil shear strain. However, this is

not compatible with the laboratory tests, which demonstrated a small percentage of damping in small strains too. Thus, it is common to add a low percentage of damping using Rayleigh and Lindsay's (1945) expressions. However, adding this amount of damping may cause overdamping in large strains. Thus, due to the suggestion of some studies and the experience of the authors, it is better not to consider viscous damping in nonlinear soil layers modeled with Masing rules because it may worsen the over-damping problems. Besides, the damping ratio of 2% is considered for the DSM pillow.

2.1. Soil domain boundaries

In order to get rational and proper response from the wave propagation problem in half-space soil domain, the reflection of the waves from boundaries should be prevented since the soil medium is infinite, and no reflection occurs from the boundaries. These non-reflecting boundaries are referred to as absorbent boundaries or transmitting boundaries in the literature. One of the most popular and useful absorbent boundaries in dynamic soil problems is Lysmer-Kuhlemeyer formulation (1969), which is utilized to model infinite soil boundaries in this paper.

In the Lysmer-Kuhlemeyer method, dashpots in all degrees of freedom are used in the boundary nodes of the soil to apply the effects of the absorbent boundaries and absorb the *S* and *P*- waves. Viscous coefficient of these dashpots is defined as Eq. (1) in which C_p is the coefficient of normal dashpots for absorbing *P*-waves, and C_s is the coefficient of tangential dashpots for absorbing *S*-waves (Lysmer and Kuhlemeyer 1969; Lysmer and Waas 1972; Rezaie at al. 2018)

$$C_p = \rho c_p A, \quad C_s = \rho c_s A \tag{1}$$

Where ρ and A are the mass density of the soil medium and the corresponding area of each dashpot, respectively, furthermore, c_p and c_s are *P*-wave and *S*-wave velocities. Besides, ABAQUS has introduced "infinite elements" for the formulation of Lysmer and Kuhlemeyer. The corresponding infinite-element for CPE4R is CINPE4, a 4-node plain strain, linear, one-way infinite element. Thus, the infinite half-space in ABAQUS software could be modeled either with Lysmer dashpots or CINPE4 elements. A schematic model of the 2D soil domain with Lysmer absorbent dashpots is illustrated in Fig. 3.

In this set of analyses, the bottom boundary is assumed to be transmitting boundary modeled with Lysmer dashpots. This model is valid for the cases that the rigidity of the bedrock is comparable with the rigidity of the soil, or the bedrock is placed at a very deep level.

The depth of the soil medium, as it is shown in the Table 1 is 150m. Furthermore, viscous vertical boundaries placed on both sides of the model should be far enough to capture the influence of parameters like natural frequency and soil characteristics and absorb waves properly. Due to Roesset and Ettouney (1977) vertical boundaries should be placed in the distance of 5B-10B (*B*=half width of DSM pillow) from the center. So, the dimension of the 2D soil model was $800m \times 150m.$

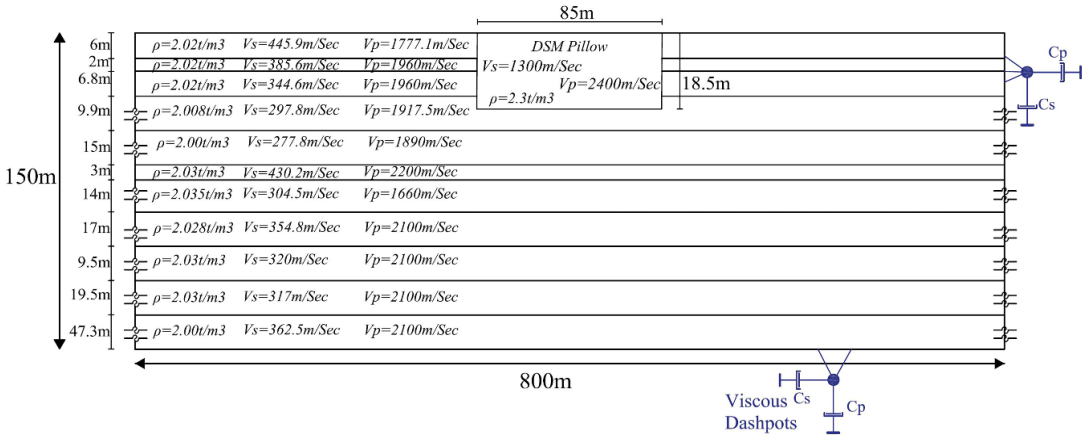

Fig. 3. Schematic soil model with DSM pillow and viscous boundaries (vertical and horizontal scales are not identical)

2.2. Input ground motions

Two categories of input ground motion are used in the nonlinear analyses, which include artificial ground motion produced from bedrock spectrums and real time histories recorded on the hard rock sites.

2.2.1. Artificial ground motions

In this study, uncertainty in the input motion is performed through generating various artificial seismic excitations to be used as input motions in analyses. These artificial input ground motions are generated using the target bedrock acceleration spectrums (bedrock Uniform Hazard Spectrum (UHS)) with a return period of 100, 475, 1000 and 10000 years, which were obtained from Seismic Hazard Analysis. These target bedrock spectrums are shown in Fig. 4 and are named as UHS100, UHS475, UHS1000 and UHS10000 in this paper.

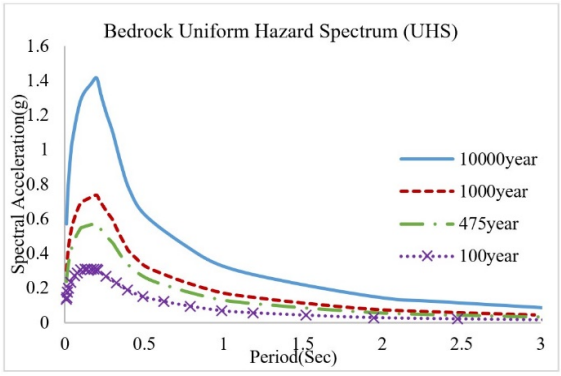

Fig. 4. bedrock Uniform Hazard Spectrum (UHS)) with a return period of 100, 475, 1000 and 10000 years

In order to make the accelerogram compatible with the specific response spectrum and to add certain statistical properties to accelerogram such as frequency content, maximum peak acceleration amplitude, artificial accelerograms are generated for the mentioned UHS. The process of generating artificial time histories was done with MATLAB (2014). The Eq. (2) is utilized for artificial earthquake generation (Gasparini and Vanmarcke 1976; Salmon and Kuilanoff 1991).

$$\ddot{u}(t) = E(t) \times \sum_{k=1}^{N} A_k \sin(\omega_k t + \phi_k) \tag{2}$$

Where A_k, ω_k and ϕ_k are the amplitude, frequency and initial phase of k^{th} harmonic acceleration, respectively. Moreover, *E(t)* is the acceleration envelope, which makes the stationary acceleration resulted from the summation of sinusoidal harmonic motions simulate the transient nature of a real accelerogram.

Since ϕ_k is generated randomly different time histories are simulated for each bedrock spectrum, four artificial accelerograms are produced for spectrum with a return period of 1000 and 10000 years (named ACC1 to ACC4) and three for spectrums with a return period of 475 and 100 years (named ACC1 to ACC3). Different characteristics of these generated motions are presented in Table 3.

Table 3 Characteristics of different motions generated for bedrock UHSs

Bedrock spectrum	Motion ID	PGA(g)	PGV(cm/Sec)	PGD(cm)
UHS1000	ACC1	0.28155	18.49899	8.58471
	ACC2	0.30334	15.82723	13.23045
	ACC3	0.30098	21.51436	27.30347
	ACC4	0.32409	16.13534	30.12789
UHS10000	ACC1	0.6136	38.58214	32.08767
	ACC2	0.6391	54.65705	83.23471
	ACC3	0.5749	43.93041	51.53109
	ACC4	0.602	52.59372	114.05489
UHS100	ACC1	0.15896	12.09019	12.09934
	ACC2	0.14522	7.3499	13.01883
	ACC3	0.14397	7.55993	12.79054
UHS475	ACC1	0.25658	12.58795	22.93406
	ACC2	0.29561	17.38518	21.6441
	ACC3	0.25168	12.51109	21.66457

2.2.2. Regular ground motions

In addition to the ground motions generated by the process mentioned in the previous part, four time-history ground motions are selected from FEMA 440 (2005). The characteristics of these time histories are presented in Table 4.

Table 4 Characteristics of real time histories used in analyses

No.	Earthquake Name	Station Name	Magnitude (Ms)	Component (Deg)	PGA ($m/\sec^2$)
1	Landers 1992	Amboy	7.5	90	1.46
2	Loma Prieta 1989	Point Bonita	7.1	297	0.714
3	Northridge 1994	LA,Wonderland	6.8	185	1.687
4	Northridge 1994	San Gabriel, E. Grand Ave.	6.8	180	2.56

2.3. Input waves in viscous nonreflecting base

In all of the analyses the semi-infinite domain laid under modeled soil medium is simulated with viscous nonreflecting bottom boundary. This viscous boundary is simulated with Lysmer dashpots in this paper. In this case, the input ground motion should be applied as normal and shear stresses (just shear stresses when SH waves are being studied) at the viscous base of the model. This shear stress is defined using Eq.(3) (Kaklamanos 2012; Lysmer and Kuhlemeyer 1969).

$$\tau(t) = \rho_r . V_{S_r} . v(t) \tag{3}$$

Where $\tau(t)$ is the shear stress, ρ_r is the density of the base, V_{S_r} is the shear-wave velocity of the base and $v(t)$ is the velocity time histories of the input ground motion. This velocity time history should be multiplied by a factor of two since half of the applied stress will be absorbed by dashpots or infinite elements, however, when the input motion is obtained from a rock outcrop recording at the ground surface, the amplitude of this motion is twice the upgoing incident wave (Kaklamanos 2012; Lysmer and Kuhlemeyer 1969). Since the artificial time histories are generated using bedrock UHS, they are assumed as incident waves. Whereas, the real earthquakes that were recorded on hard rock site, are assumed as outcropping motions. It should be noted that real time histories are not scaled.

3. Verification

In every numerical modeling, to achieve precise responses and to ensure the accuracy of the modeling procedure, it is necessary to validate the developed model with other verified models. In this part, the accuracy of modeling soil material with parallel elements is verified through nonlinear analysis of the soil. For this purpose, we used models available in the Ph.D. dissertation with title of “Quantifying Uncertainty in Earthquake Site Response Models Using the KiK-net Database” submitted by James Kaklamanos (2012) and the related paper “A Simple Approach to Site-Response Modeling: The Overlay Concept” by James Kaklamanos et al. (2015a). The soil response of IWTH08 station site in the Kiban-Kyoshin network in Japan (KiK-net) was calculated using the overlay method, which uses the concept of parallel elements.

A 1-D soil response analysis was carried out using C3D8R elements with unit ($1m \times 1m$) cross-section. The input ground motion had a moment magnitude of 6.8, which occurred on 24th July 2008.

This one-dimensional soil domain is modeled 2-D in this verification process since the nature of the models studied in this paper necessitated authors to use full 2-D analysis with CPE4R elements. The model has the same 100m overall depth. The results obtained for 5% damped pseudo-acceleration response spectra for the surface ground motion and stress-strain hysteresis curve in the mid-depth of the first layer at the depth of 2m are illustrated in the Fig. 5. It can be seen from Fig. 5 that there is a good fitness between the results obtained from 2D model constructed in this study and one dimensional analysis carried out Kaklamanos (2012) and observed site response. The small differences between results obtained from the model constructed in this study and one dimensional analysis carried out Kaklamanos (2012) might be due to the fact that the model of this study is 2D and it has two-dimensional behavior while the model of the mentioned paper is 1D. Therefore, it could be concluded that the models used in this study are efficient.

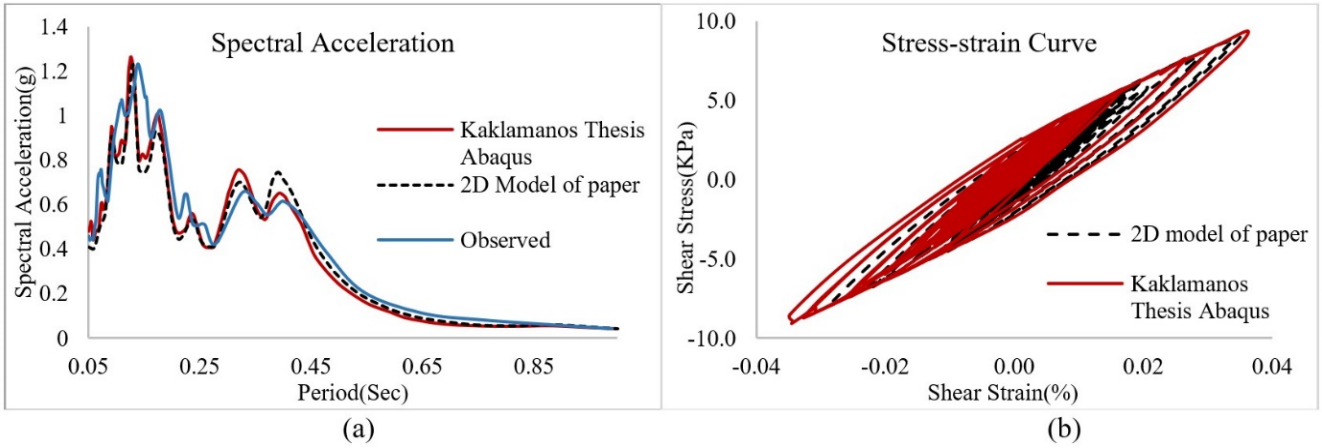

Fig. 5. a) Acceleration response spectrum obtained from Kaklamanos (2012) FE model of this paper and observed surface motion, b) Shear stress-shear strain loops of Kaklamanos (2012) model and FE analysis model

4. Results and discussion of DSM block with specific properties

In this part of the paper, results obtained from fully nonlinear site response analyses with and without DSM enhancing pillow are demonstrated. In the first part of the result section, the surface response acceleration time histories are studied to investigate the possible effects of soil treatment with block type DSM on acceleration of surface of soil domain. The second part is devoted to the effects of this improved soil on the pseudo-acceleration spectrum of the surface of the soil layers. In the last part, the stress-strain hysteresis loops of models are compared to clarify the exact impact of the enhanced soil on nonlinear behavior of the soil layers.

4.1. Surface response acceleration time histories

Fig. 6, Fig. 7 and Fig. 8 demonstrate the surface accelerations for input time histories generated from UHS1000, UHS10000 and UHS100, respectively. The amounts of PBAs (peak base accelerations) and PSAs (peak surface accelerations) for improved and unimproved soil are demonstrated in the Table 5 for all time histories. For UHS1000, the PBAs are 0.2815g, 0.3033g, 0.30098g and 0.32409g for ACC1 to ACC4, respectively. These base motions are affected from de-amplification effects of the soil layers while travelling to the surface of the ground. Therefore, the PSAs of the soil layer are 0.239g, 0.282g, 0.24g and 0.261g for ACC1 to ACC4; however, by improving soil with DSM, these amounts reduce to 0.104g, 0.1115g, 0.1053g and 0.1128g. The overall average reduction is 57% (See Fig.6 and Table 5).

The response surface accelerations for time histories generated from UHS10000 are shown in Fig. 7. The PBAs are 0.6136g, 0.6391g, 0.5749g and 0.602g for ACC1 to ACC4, respectively. The PSAs before enhancing soil are equal to 0.32g, 0.2658g, 0.268g and 0.298g. These results which are obtained from conducted site response analyses, demonstrate a very considerable amount of de-amplification that all of the motions generated from UHS10000 have undergone while traveling through the soil layers. After improving soil, these amounts with an average reduction of 52% reach 0.144g, 0.137g, 0.141g and 0.129g for ACC1 to ACC4, respectively. On the other hand, the PSAs for input motion with UHS100, which are equal to 0.164g, 0.153g and 0.149g, have an overall reduction of 50% and reach to 0.08g, 0.071g and 0.075g (shown in Fig. 8). In these motions, the PBAs are 0.16g, 0.145g and 0.144g for ACC1 to ACC3, respectively.

The outcomes of the analyses with real outcropping earthquakes are shown in Fig. 9 and Table 6. For the Landers ground motion with PBA=0.1461g, the PSA is 0.102g. By improving soil, this amount decreases to 0.058g. The peak surface response acceleration of the Loma-Prieta earthquake with PBA=0.0735g is 0.051g, while this amount reduces to 0.0404g after using the DSM method in the soil and has a 21% reduction. For the Northridge-LA-Wonderland as the input motion with PBA=0.159g, the PSA is 0.157g and after improving soil, this amount reduces to 0.075g. Finally, when the input motion is Northridge-San Gabriel with PBA=0.1417g, the peak surface acceleration is equal to 0.12g, which reduces 44% and is equal to 0.065g after enhancing soil in the FE model.

Table 5 Peak base and surface accelerations of unimproved and improved soil for different artificial input motions

Bedrock UHS	Time histories	PBA(g)	PSA(g)- Original soil	PSA(g)- Enhanced with DSM	Reduction(%)
UHS1000	ACC1	0.2815	0.239	0.104	56
	ACC2	0.3033	0.282	0.1115	60
	ACC3	0.301	0.240	0.1053	56
	ACC4	0.324	0.261	0.1128	57
UHS10000	ACC1	0.6136	0.32	0.144	55
	ACC2	0.6391	0.2658	0.137	48
	ACC3	0.5749	0.268	0.141	47
	ACC4	0.602	0.298	0.129	57
UHS100	ACC1	0.159	0.164	0.08	52
	ACC2	0.145	0.153	0.071	54
	ACC3	0.144	0.149	0.075	49
UHS475	ACC1	0.2566	0.226	0.1	56
	ACC2	0.2956	0.225	0.097	57
	ACC3	0.2516	0.229	0.1	56

Table 6 Peak base and surface accelerations of unimproved and improved soil for scaled real input motions

Outcropping real ground motion	PBA(g)	PSA(g)- Original soil	PSA(g)- Enhanced with DSM	Reduction (%)
Landers-Amboy	0.1461	0.102	0.058	43
Loma Priet-Point bonita	0.0735	0.051	0.0404	21
Northridge-LA-Wonderland	0.159	0.157	0.075	52
Northridge-San Gabriel	0.1417	0.12	0.065	44

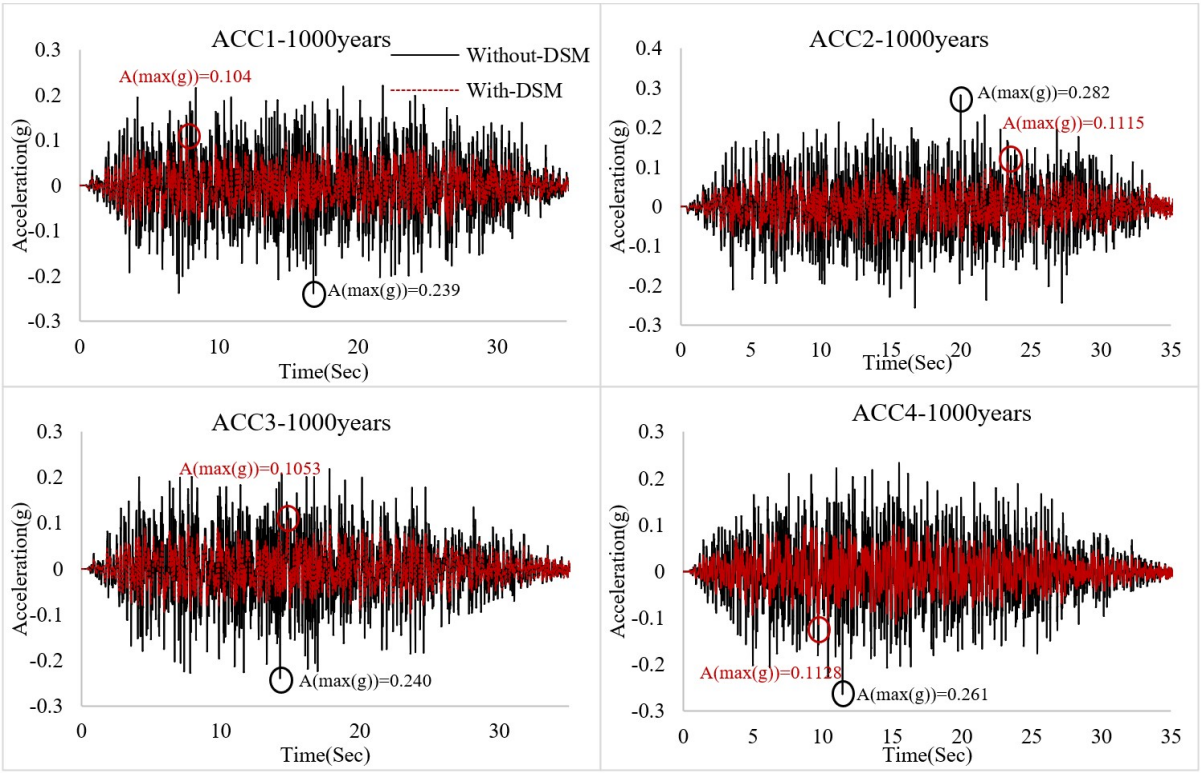

Fig. 6. Surface response acceleration time histories for ACC1 to ACC4, generated from UHS1000.

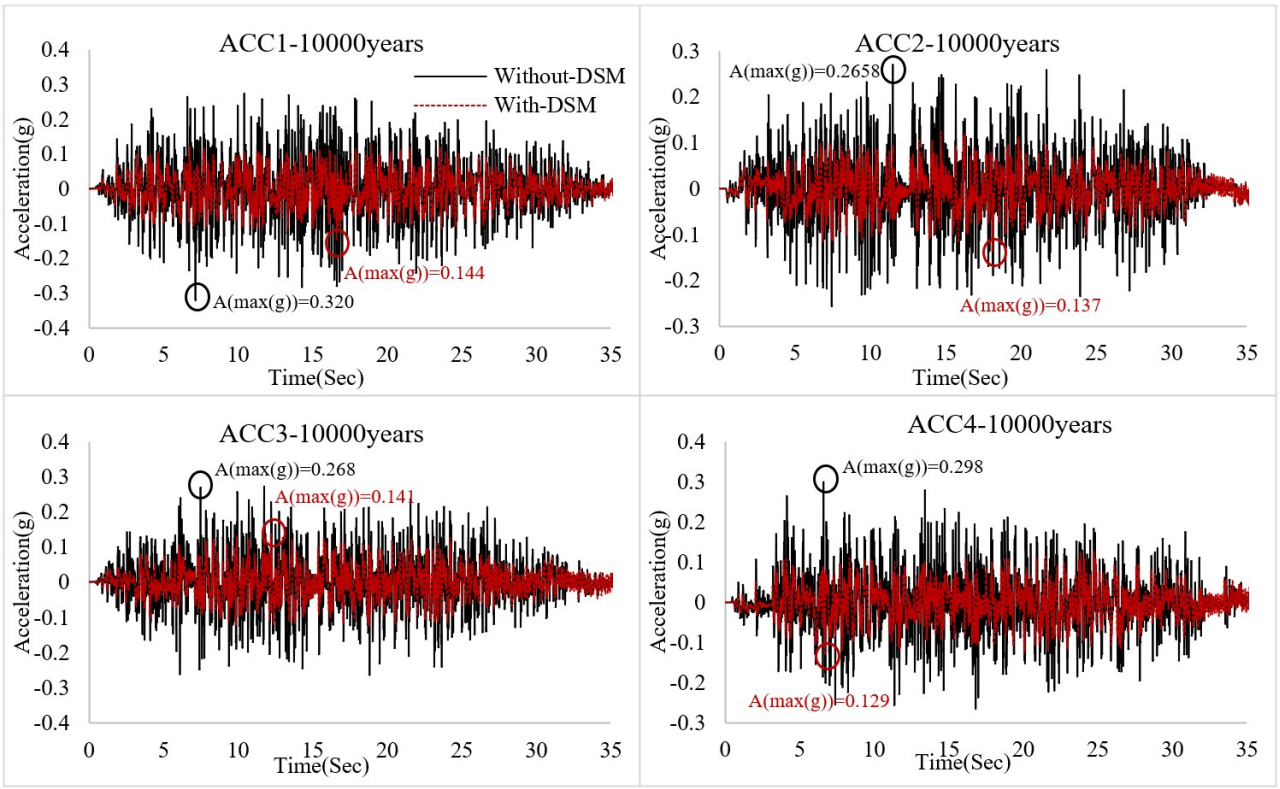

Fig. 7. Surface response acceleration time histories for ACC1 to ACC4, generated from UHS10000.

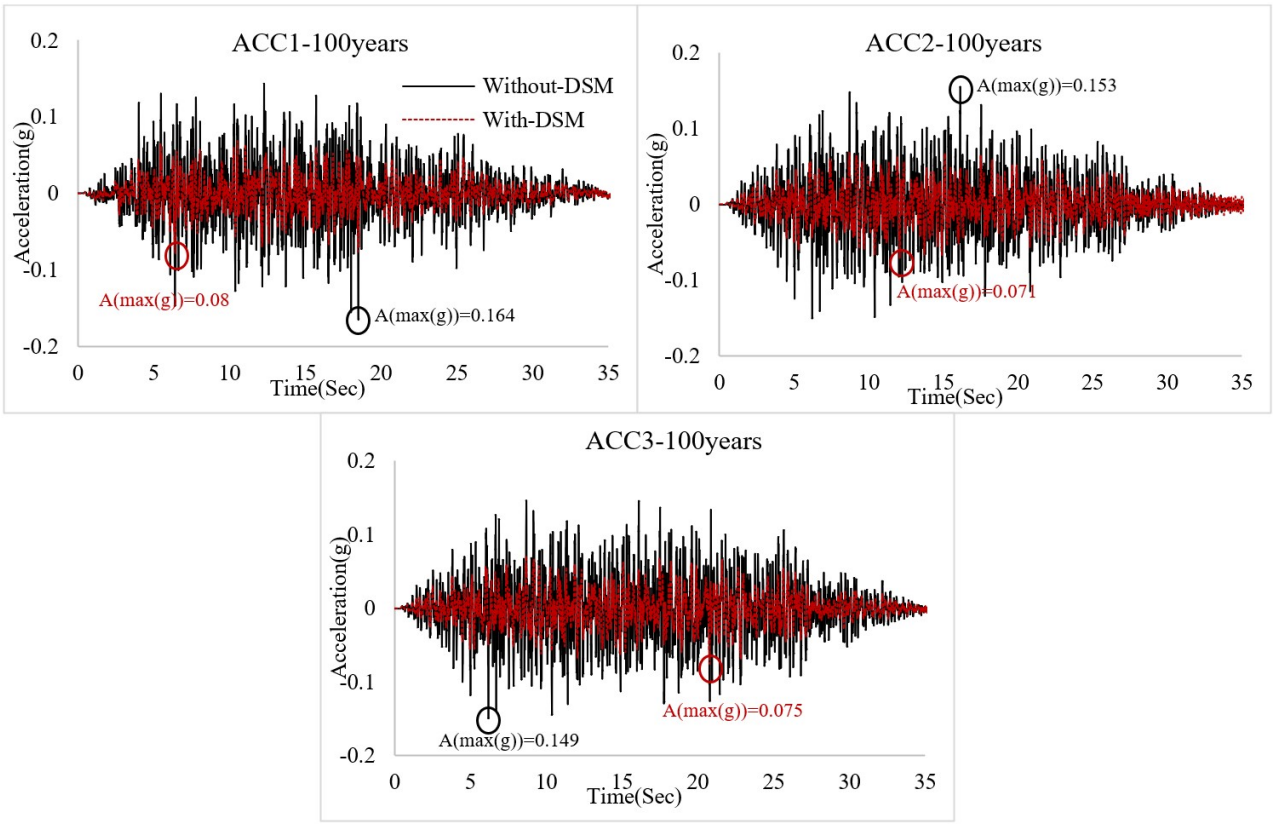

Fig. 8. Surface response acceleration time histories for ACC1 to ACC3, generated from UHS100.

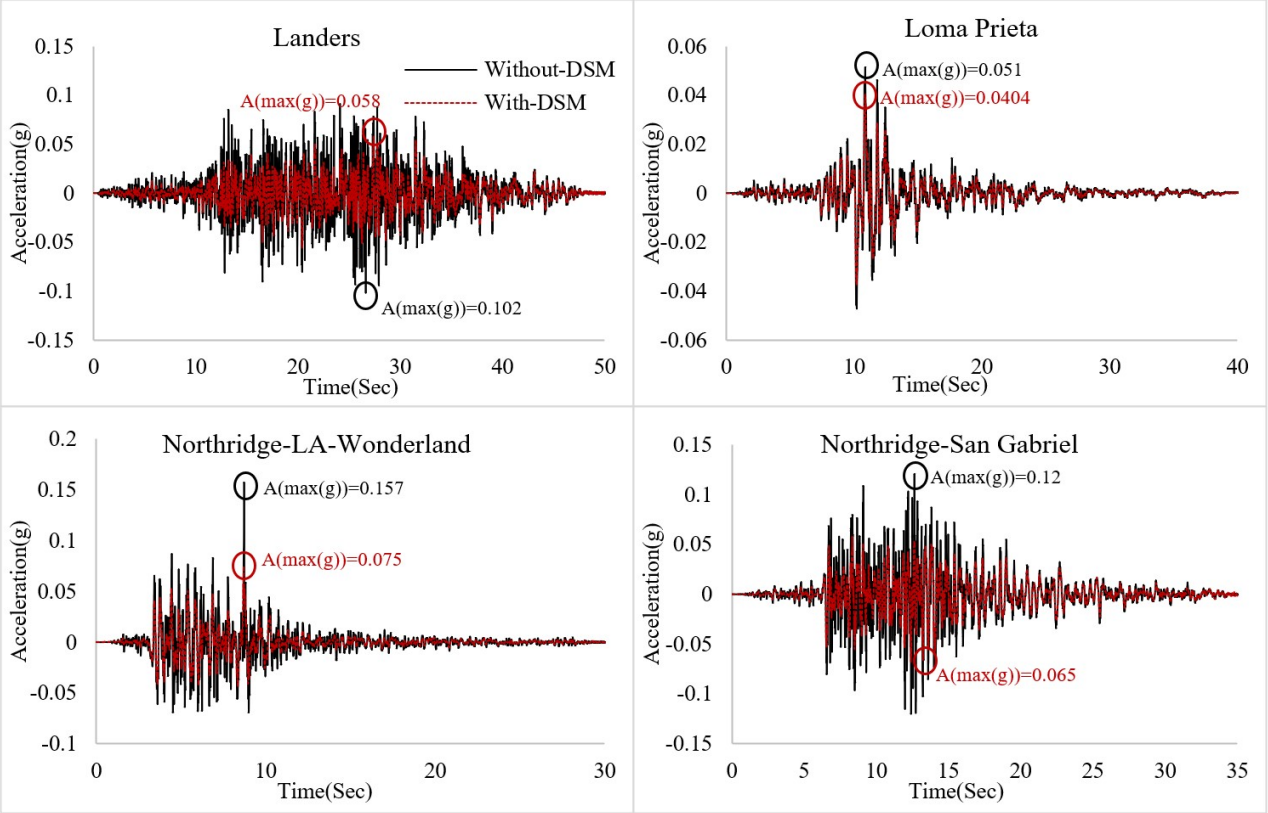

Fig. 9. Surface response acceleration time histories for real ground motions.

4.2. Surface spectral response acceleration

The 5%-damped acceleration response spectra for the surface ground motions are shown in Fig. 10 for the models with base motion created from bedrock spectrum with 1000 years return period (UHS1000). It can be seen from the spectrums that improving soil has a very positive effect in reducing spectral response acceleration up to the period of approximately 0.7 seconds after this period and especially in periods greater than 1 second, the difference between the two spectrums is about zero. The average reduction for periods smaller than 0.7 seconds is about 30%, while the maximum reduction is 60-70%. Also, the overall average reduction for all period range is 4.5%.

As the surface acceleration response spectra for the models with input motions ACC1 to ACC4 produced from UHS10000 are illustrated in Fig. 11, it can be seen that similar results with Fig. 10 are obtained for these analyses. In this case, using the DSM pillow results in the maximum amount of reduction of approximately 65-75%; however, the average amount of reduction for periods smaller than 0.7 seconds is 27%.

Fig. 12 depicts the 5%-damped acceleration response spectra for the surface ground motions for real outcropping input motions. When the input motion is the Landers time histories, it is observed that enhancing soil leads to an average reduction of 26% in spectral acceleration for periods smaller than 0.75 seconds. After this period, the positive effects of using DSM vanishes and almost the same spectral accelerations are obtained for improved and unimproved soil. In this case, the maximum reduction in spectral acceleration is 60%. Whereas, for the analysis with the Loma Prieta time histories, the positive effect of improving the soil in decreasing spectral acceleration disappears after a smaller period of 0.6 seconds. For this ground motion, the maximum reduction in spectral acceleration is 40% and the average reduction is 20% for periods shorter than 0.6 seconds. For two ground motions of Northridge-LA-Wonderland and Northridge-San Gabriel, utilizing the DSM results in approximately 60% smaller peak spectral acceleration. The difference between spectral acceleration of improved and unimproved soil is less than 5% for periods greater than 0.7 seconds. Moreover, the average spectral acceleration reduction for periods smaller than 0.7 seconds is 25%.

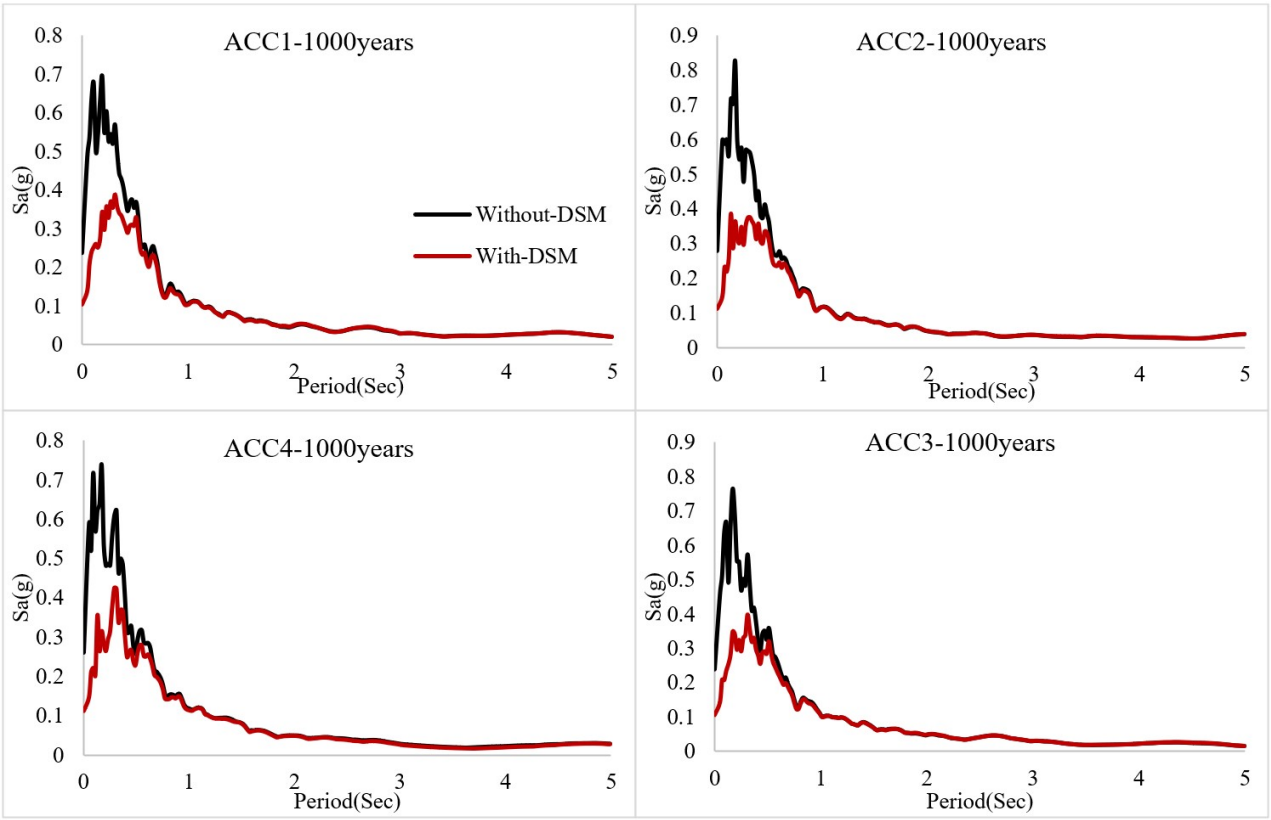

Fig. 10. Surface spectral response accelerations Sa(g) for ACC1 to ACC4, generated from UHS1000.

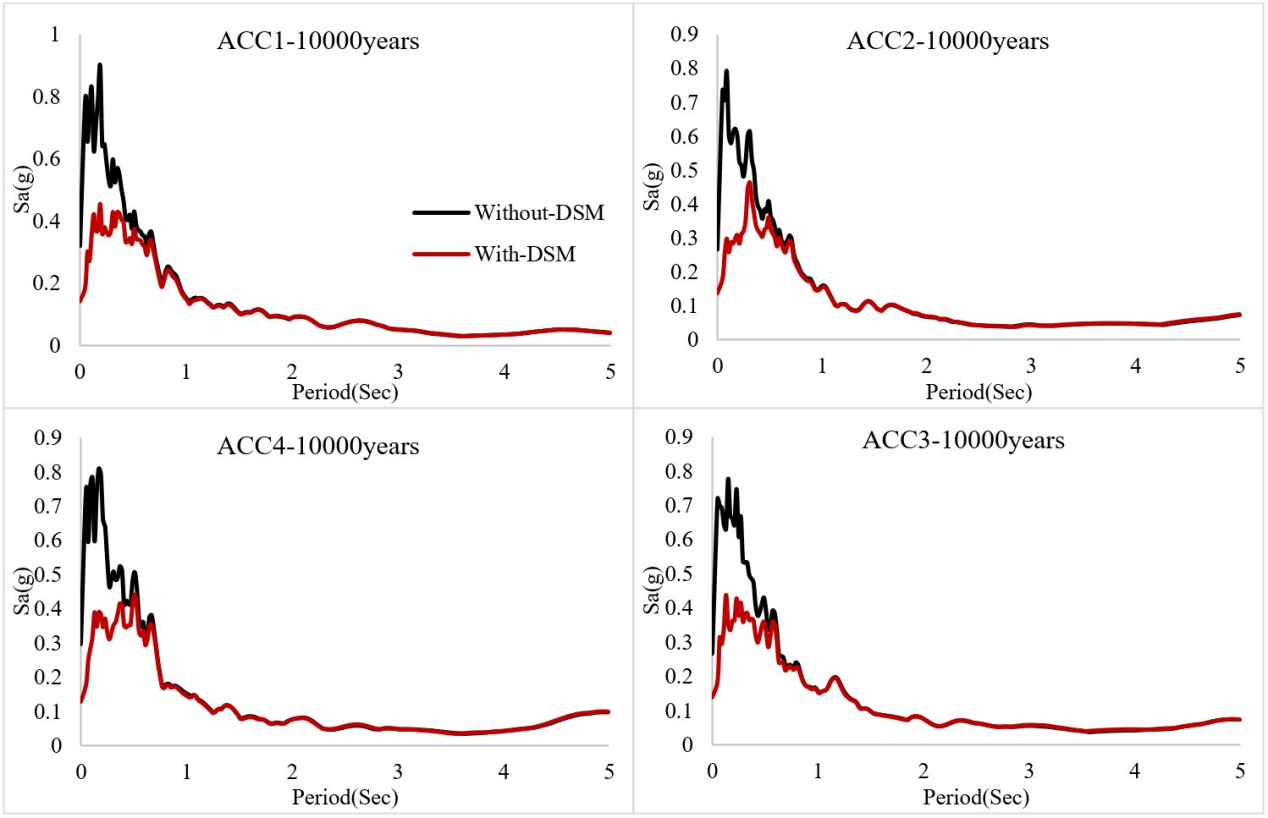

Fig. 11. Surface spectral response accelerations Sa(g) for ACC1 to ACC4, generated from UHS10000.

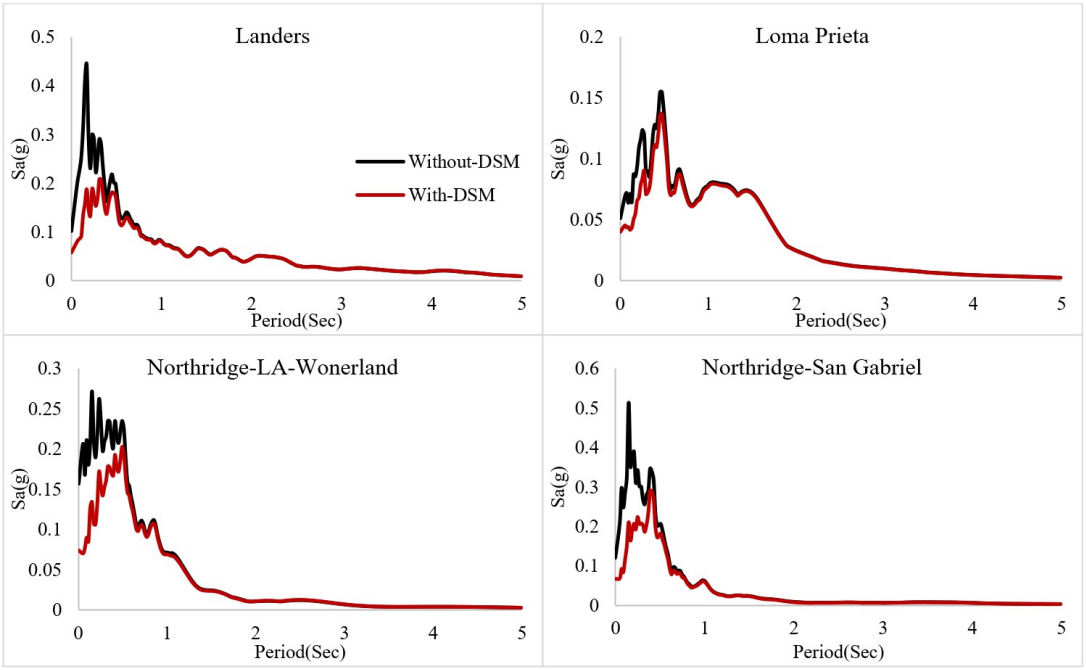

Fig. 12. Surface spectral response accelerations Sa(g) for outcropping real motions.

4.3. Shear stress-shear strain hysteresis loops

The shear stress- shear strain hysteresis loops at the mid-point of layer 1 and at the top of layer 4, according to Table 1, for UHS1000 and UHS10000 are illustrated in Fig. 13 and Fig. 14 (Sample of results obtained from different input time histories are depicted in these figures since the results of different time histories are similar). The first columns of these figures are related to the point with H=3m and the second is related to H=14.8m. For both UHS1000 and UHS10000, it can be seen that in the point with 3m depth (middle of the first layer), the soil has undergone a very limited nonlinearity and its behavior is almost linear. The reason for this limited width loop in UHS10000 might be the significant de-amplification effect that occurred within the soil layers of this site in this level of ground motion. In both cases of UHS1000 and UHS10000, it can be observed that by improving the soil amounts of strain decrease significantly. As it was expected, there is a considerable increase in the stiffness after using the DSM. For UHS1000, stress varies between -8 to 8 kPa for unimproved soil and between -4 to 4 kPa for improved soil. For UHS10000, these amounts are -10 to 10 kPa and -6 to 6 kPa for unimproved and improved soil, respectively.

On the other hand, wider stress-strain loops are generated for H=14.8m as it is illustrated in the second column of Fig. 13 and Fig. 14 for UHS1000 and UHS10000, respectively. In this depth, the soil has undergone a large nonlinearity for both levels of input motion. Even though a significant amount of de-amplification occurs when the input motion is stronger and generated from UHS10000, the corresponding loops are wider. For the point with depth 14.8m, the stress is between -50 to 50 kPa for UHS10000, while this amount is between -30 to 30 for UHS1000 for both improved and unimproved soil. It should be noted that in both depths and for both levels of ground motions the behavior of improved soil is almost linear (the probable reasons of this behavior is related to Mohr-Coulomb criterion used to model DSM pillow and high shear strength which is related to the high cohesion of the improved soil (C)).

In the analyses with motions created from UHS100 for points with depth 3m and 14.8m, very limited nonlinearity is observed (in the point H=3m the behavior of unimproved soil is almost linear and for the point with H=14.8m loops with a very limited width are generated). As it is illustrated in Fig. 15 for UHS100, stiffness increases and the strain has a significant reduction when the DSM pillow is used.

The hysteresis loops of the models with real outcropping earthquakes as input base motion are depicted in Fig. 16. The behavior of the midpoint of the first layer (H=3m) is almost linear for all of these outcropping motions. In this case, using DSM increases the stiffness and reduces the amounts of strain considerably. Whereas the behavior of the point H=14.8m is nonlinear in all outcropping motions, but the width of the loop is different for these motion. For Loma-Prieta motion, a loop with a very limited width is generated while for other motions, hysteresis loops are wider. Since the material of the soil layers is constant in all of the models, the width of the loops depends on the intensity of the motion and amplification or de-amplification effects of the soil layer on each motion. Similar to the H=3m in H=14.8m, the behavior is almost linear for enhanced soil.

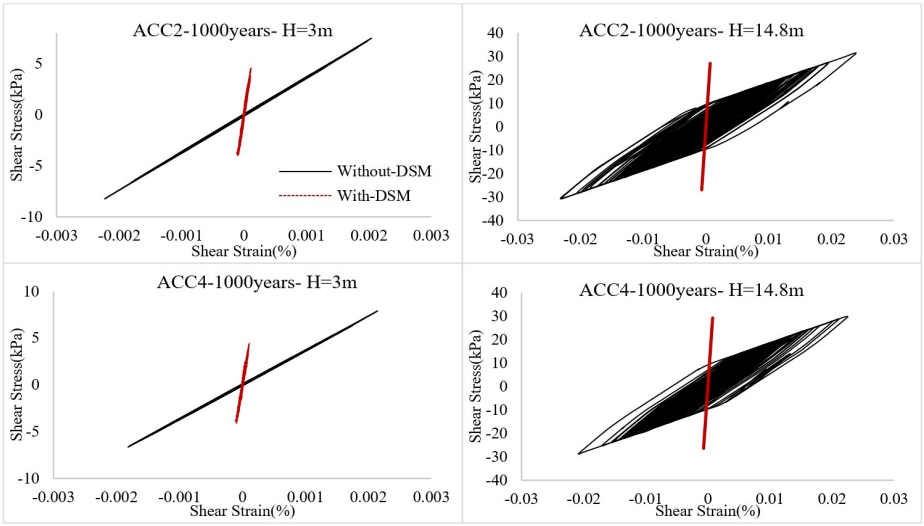

Fig. 13. Shear stress- shear strain hysteresis loops for motions generated from UHS1000, (a) H=3m, (b) H=14.8m

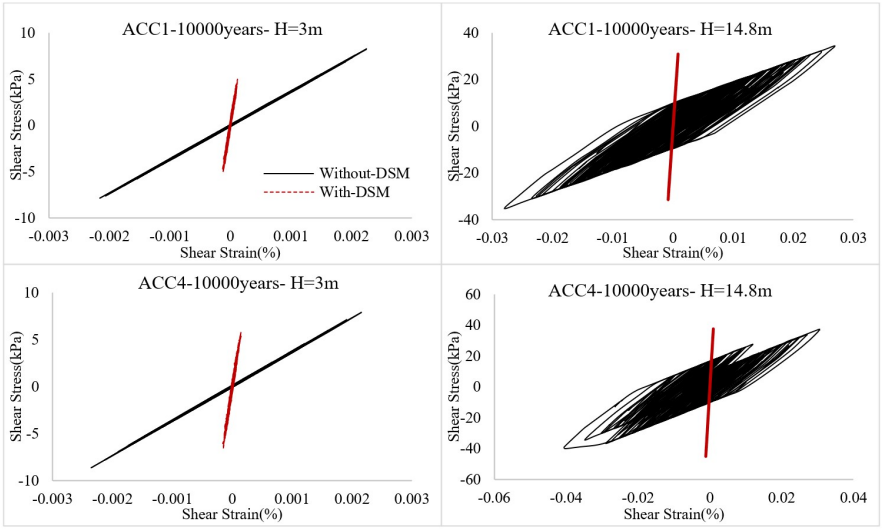

Fig. 14. Shear stress- shear strain hysteresis loops for motions generated from UHS10000, (a) H=3m, (b) H=14.8m

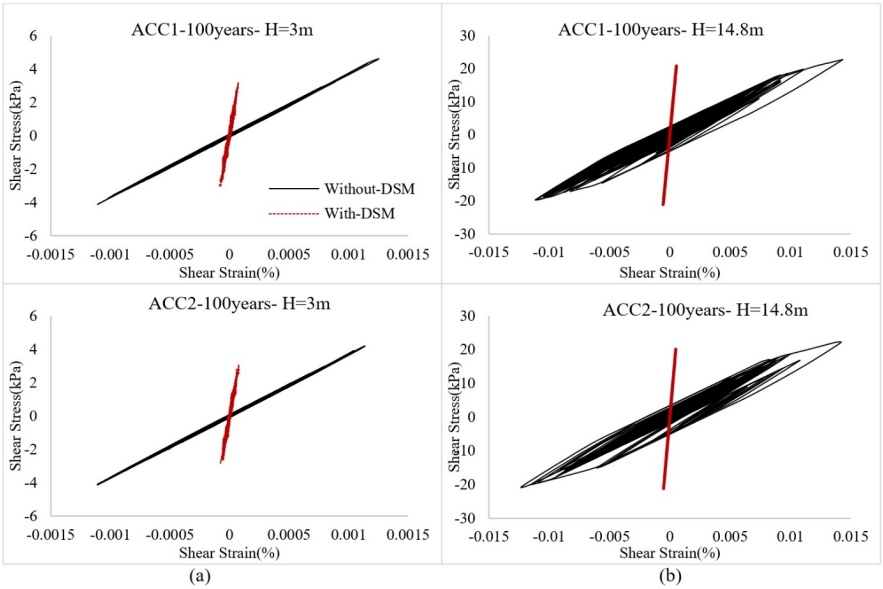

Fig. 15. Shear stress- shear strain hysteresis loops for motions generated from UHS100, (a) H=3m, (b) H=14.8m

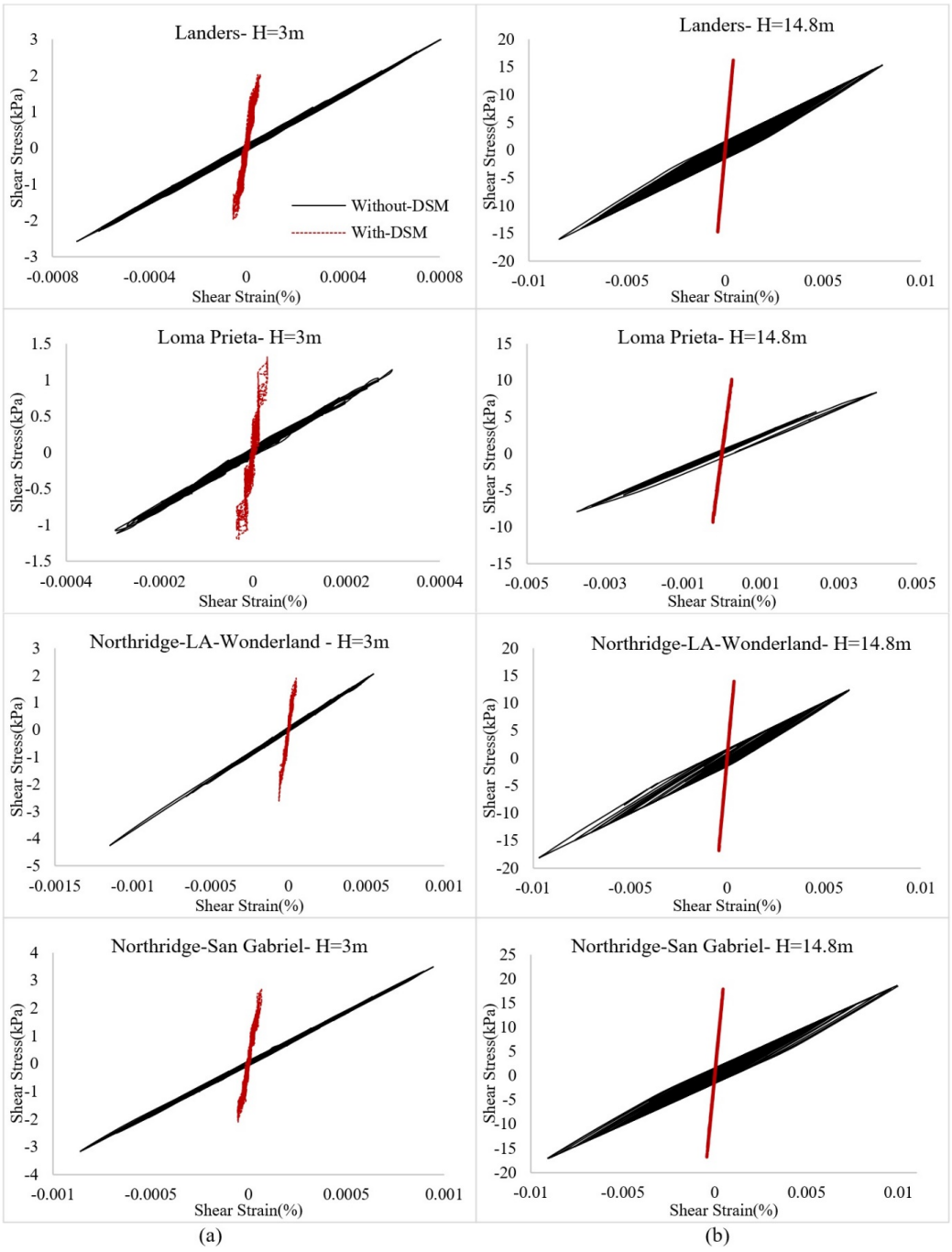

Fig. 16. Shear stress- shear strain hysteresis loops for real time histories, (a) H=3m, (b) H=14.8m

5. Conclusion

The effects of using block type deep soil mixing treatment on the seismic behavior of the soil layers and site response of a specific site are studied in this investigation through fully nonlinear dynamic analyses. Lysmer absorbing boundaries are used to model the semi-infinite medium around the modeled soil layers. Two sets of artificial and real input ground motion are selected for analyses. The most significant results obtained from nonlinear time-domain analyses are as follows:

- Improving soil with soil-cement block type mixture has a positive effect on the acceleration response of the ground surface. The surface response acceleration has a 45-60% decrease after enhancing soil for models with artificial input motion generated from the uniform hazard spectrum of the site. When real ground motions are used as input waves, surface accelerations decrease 22-50% after improving the soil.
- The input ground motion has undergone considerable de-amplification traveling through different layers of soil, especially in strong motions.

- The positive effects of improving the soil regarding the spectral acceleration are considerable in periods smaller than 0.7-1 Sec for different artificial and real input motions. In this range of periods, the average reduction in spectral acceleration is 20-30% for different motions. However, for periods bigger than these amounts, this positive effect vanishes, and for a wide range of periods (bigger than 1Sec), the differences in the spectral acceleration of unimproved and improved soil are almost zero. The maximum amount of reduction in spectral acceleration for different input motions after utilizing the DSM pillow varies between 40% and 70%, which are very considerable amounts.
- Using the overlay model (parallel elements) in modeling nonlinear behavior of soil material resulted in a very proper generation of shear stress-shear strain hysteresis loops of different depth of the soil domain.
- Stiffness of the soil layers are increased after improving the soil with block type DSM which is expected due to the high stiffness of cementitious material used in the treatment, and this leads to a more stable soil and less settlements; however; the cost of this type of DSM is higher because of the higher volume of improvement but nevertheless much cheaper compared to the conventional base isolation.

Author contributions: Writing & editing, MM Shaghaghi; Conceptualization, MM Shaghaghi, IM Kani, H Yousefi; Methodology, MM Shaghaghi; Supervision, IM Kani; Advising, H Yousefi.

Editor: Pablo Andrés Muñoz Rojas.

Reference

Alford RM, Kelley KR, Boore DM (1974) Accuracy of finite difference modeling of the acoustic wave equation. Geophysics 39:834–842. https://doi.org/10.1190/1.1440470

Bolisetti C (2014) Site response, soil-structure interaction and structure-soil-structure interaction for performance assessment of buildings and nuclear structures. Ph.D. dissertation, State University of New York.

Bolisetti C, Whittaker AS, Mason HB, Almufti I, Willford M (2014) Equivalent linear and nonlinear site response analysis for design and risk assessment of safety-related nuclear structures. Nuclear Engineering and Design 275:107-121. https://doi.org/10.1016/j.nucengdes.2014.04.033

Bradley BA, Araki K, Ishii T, Saitoh K (2013) Effect of lattice shaped ground improvement geometry on seismic response of liquefiable soil deposits via 3-D seismic effective stress analysis. Soil Dyn Earthq Eng 48:35-47. http://dx.doi.org/10.1016/j.soildyn.2013.01.027

Fares R (2019) Modeling techniques for building design considering soil-structure interaction. Ph.D. dissertation, Université Côte d'Azur, Nice, France.

FEMA-440 (2005) Recommended provisions for improvement of nonlinear static seismic analysis procedures. Federal Emergency Management Agency (FEMA), Washington, D.C., USA.

FHWA-RD-99-138 (2000) An Introduction to the Deep Soil Mixing Methods as Used in Geotechnical Applications. Federal Highway Administration (FHWA), McLean, V.A., USA.

FHWA-HRT-13-046 (2013) Federal Highway Administration Design Manual: Deep Mixing for Embankment and Foundation Support. Federal Highway Administration (FHWA), McLean, V.A., USA.

Gasparini D, Vanmarcke EH (1976) Simulated Earthquake Motions Compatible with Prescribed Response Spectra. Constructed Facilities Division, Dept. of Civil Engineering, Massachusetts Institute of Technology, Massachusetts, USA.

Hashash YMA, Phillips C, Groholski DR (2010) Recent advances in non-linear site response analysis. Proceeding of 5th International Recent Advances in Geotechnical Earthquake Engineering and Soil Dynamics, San Diego, California, USA.

Iwan WD (1967) On a Class of Models for the Yielding Behavior of Continuous and Composite Systems. J Appl. Mech. 34(3):612-617. https://doi.org/10.1115/1.3607751

Kaklamanos J (2012) Quantifying uncertainty in earthquake site response models using the Kik-Net database. Ph.D. dissertation in Civil and Environmental engineering, Tuft University, Massachusetts, USA.

Kaklamanos J, Dorfmann L, Baise LG (2014) Modeling dynamic site response using the overlay concept. Geo-Congress 2014 Technical Papers: Geo-Characterization and Modeling for Sustainability, Atlanta, Georgia, USA, February.

Kaklamanos J, Dorfmann L, Baise LG (2015a) A Simple Approach to Site-Response Modeling: The Overlay Concept. Seismological Research Letters 86(2A):413-423.

Kaklamanos J, Baise LG, Thompson EM, Dorfmann L (2015b) Comparison of1D linear, equivalent linear, and nonlinear site response models at six KiK-net validation sites. Soil Dyn Earthq Eng 69:207-219. http://dx.doi.org/10.1016/j.soildyn.2014.10.016

Khosravi M, Boulanger RW, Tamura S, Wilson DW, Olgun CG, Wang Y (2016) Dynamic Centrifuge Tests of Soft Clay Reinforced by Soil–Cement Grids. J Geotech Geoenviron Eng ASCE 142(7):04016027. http://dx.doi.org/10.1061/(ASCE)GT.1943-5606.0001487

Kitazume M, Terashi M (2013) The Deep Mixing Method. Taylor & Francis Group, CRC Press, London, UK.

Kramer SL (1996) Geotechnical Earthquake Engineering. Prentice Hall, Upper Saddle River, New Jersey, USA.

Liu SY, Du YJ, Yi YL, Puppala AJ (2012) Field Investigations on Performance of T-Shaped Deep Mixed Soil Cement Column–Supported Embankments over Soft Ground. J Geotech Geoenviron Eng ASCE 138(6):718-727. http://dx.doi.org/10.1061/(ASCE)GT.1943-5606.0000625

Lysmer J and Kuhlemeyer RL (1969) Finite dynamic model for infinite media. J Eng Mech Div ASCE 95:859–77.

Lysmer J, Waas G (1972) Shear waves in plane infinite structures. J Eng. Mech. Div. ASCE 98:85–105.

Masing G (1926) Eigenspannungen and verfertigung beim messing. Proceeding of 2nd International Congress on Applied Mechanics, Zurich, Switzerland.

MATLAB R2014b (2014) The MathWorks Inc., Massachusetts, USA.

Mroz Z (1967) On the description of anisotropic workhardening. J Mech Phys Solid 15:163-175.

Namikawa T, Koseki J, Suzuki Y (2007) Finite element analysis of lattice-shaped ground improvement by cement-mixing for liquefaction mitigation. Soils and Foundations 47(3):559-576. https://doi.org/10.3208/sandf.47.559

Nelson RB, Dorfmann A (1995) Parallel elasto-plastic models of inelastic material behavior. J Eng Mech 121(10):1089-1097.

O'Rourke TD, McGinn, AJ (2006) Lessons Learned for Ground Movements and Soil Stabilization from the Boston Central Artery. J Geotech Geoenviron Eng ASCE 132(8):966-989. http://dx.doi.org/10.1061/(ASCE)1090-0241(2006)132:8(966)

Rayleigh JWS, Lindsay RB (1945) The Theory of Sound, Dover Publications. New York, USA.

Rezaie A, Rafiee-Dehkharghani R, Dolatshahi KM, Mirghaderi SR (2018) Soil-buried wave barriers for vibration control of structures subjected to vertically incident shear waves. Soil Dyn Earthq Eng 109:312-323. https://doi.org/10.1016/j.soildyn.2018.03.020

Roesset JM, Ettouney MM (1977) Transmitting boundaries: a comparison. Int J Numer Anal Methods Geomech 1:151–76. http://dx.doi.org/10.1002/nag.1610010204

Salmon MW, Kuilanoff G (1991) Generation of artificial earthquake time histories for seismic design in Hanford. Proceeding of 3rd DOE Natural Phenomena Hazards Mitigation Conference, Washington, D.C., USA.

Simulia Abaqus 6.18 documentation (2018). Dassault Systems SIMULIA Corporation.

Thompson EM, Baise LG, Tanaka Y, Kayen RE (2012) A taxonomy of site response complexity. Soil Dyn Earthq Eng 41:32-43. http://dx.doi.org/10.1016/j.soildyn.2012.04.005

Yamashita K, Shigeno Y, Hamada J, Chang DW (2018) Seismic response analysis of piled raft with grid-form deep mixing walls under strong earthquakes with performance-based design concerns. Soils and Foundations 58(1):65-84. https://doi.org/10.1016/j.sandf.2017.12.002

Yapage NNS, Liyanapathirana DS, Poulos HG, Kelly RB, Leo CJ (2015) Numerical Modeling of Geotextile-Reinforced Embankments over Deep Cement Mixed Columns Incorporating Strain-Softening Behavior of Columns. Int J Geomech ASCE 15(2):04014047. https://doi.org/10.1061/(ASCE)GM.1943-5622.0000341

Zalachoris G, Rathje EM (2015) Evaluation of One-Dimensional Site Response Techniques Using Borehole Arrays. *J* Geotech Geoenviron Eng ASCE 141(12):04015053. https://doi.org/10.1061/(ASCE)GT.1943-5606.0001366